

MODES OF OSCILLATION IN A HIGH PRESSURE MICROPLASMA DISCHARGES *

Rajib Mahamud[‡], Mostafa Mobli, Tanvir I. Farouk

*Department of Mechanical Engineering
University of South Carolina, Columbia
South Carolina, USA*

Abstract

Atmospheric pressure microplasma devices, have been the subject of considerable research during the last decade. Most of the operation regime of the discharges studied fall in the ‘abnormal’, ‘normal’ and ‘corona’ modes – increasing and a ‘flat’ voltage current characteristics. However, the Negative Differential Resistance (NDR) regime at atmospheric and high pressures has been less studied and possesses the unique characteristics that can be employed for novel applications. The NDR regime has been studied for low pressure systems and has been characterized to be associated to relaxation oscillation only. In this work we report a detailed study on the different modes of self oscillation in high pressure micro plasma discharges. Detailed 2D numerical simulation has been conducted with a validated model. Predictions and experimental measurements are found to be in favorable agreement. The different self-pulsing modes of oscillation have been identified as, relaxation oscillation having medium to low frequency oscillation at low discharge current and high frequency free running oscillation at comparatively high current condition. In the relaxation oscillation, the discharge switches between a dark and glow like discharge, whereas in the free running mode the transition is observed to occur within glow like modes. These two modes of oscillation are found to be more prevalent at higher pressure. Depending on pressure, the frequency of relaxation and free running oscillations are in the kHz - MHz and MHz - GHz range respectively. External parameters influencing these self oscillations are studied.

I. INTRODUCTION

There is a recent interest towards the use of high pressure non-thermal micro discharge due to its advantages over its low pressure counterpart. Typical drawbacks of low pressure plasma discharge are the necessity of vacuum pumps, low rate of deposition or etching for CVD techniques and size restriction [1-4]. The

non-thermal micro plasma devices also has an increasing trends of application in biomedical applications [5, 6], thin film deposition [7] and surface treatment [8, 9]. Though the benefits of atmospheric or higher pressure plasma are well known, it possess significant challenges [3, 10]. The increase of collisions, viscosity and temperature at high pressure causes instability and leads to thermal plasma and streamer formation. These instabilities are non-desirable as it leads to non-uniform deposition in CVD techniques or may reach the temperature limitation of the system.

The fundamental basis of micro plasma discharge is the Paschen curve (Pressure \times interelectrode distance = constant). In most cases these discharges operate on the right side of the Paschen minimum. At the right side of the Paschen curve, a smaller field distortion can trigger instability. For a micro-hollow cathode (MHC) configuration this type of instability is experimentally observed and is identified as a relaxation type of oscillation [11, 12]. A two-dimensional fluid model has been employed to simulate MHC discharge and to numerically investigate the instability. The model predicted a self-pulsing relaxation mode [13]. However most of these studies were performed for low pressure condition and high pressure oscillatory discharge remain unexplored. The importance of external circuit parasitic capacitance on high pressure plasma discharge stability was investigated recently [14]. Configurations identical to Staack et al. [14] was numerically simulated by Farouk et al. [15] and the instability was identified to be subnormal oscillations. For a low pressure plasma discharges the subnormal oscillation has always been attributed to an instability resulting when the power circuit time constant becomes comparable to the ion transit time [16]

Understanding the phenomenon of subnormal oscillation along with ionization and chemical reaction at high pressure is important for the successful design of micro plasma devices. In the present study the self pulsing mode of a high pressure micro-plasma discharge operating in He/N₂ feed gas has been investigated to study

* Work supported by DARPA under Army Office (ARO) Grant No. W911NF1210007

[‡] email: mahamud@email.sc.edu

the effect of pressure on the self pulsing mode. The different oscillatory mode is characterized. To obtain detailed insight a two-dimensional axisymmetric plasma model has been developed consisting of 10 species and 41 step reaction kinetic mechanism. Simulations were conducted employing the COMSOL Multiphysics software package [17].

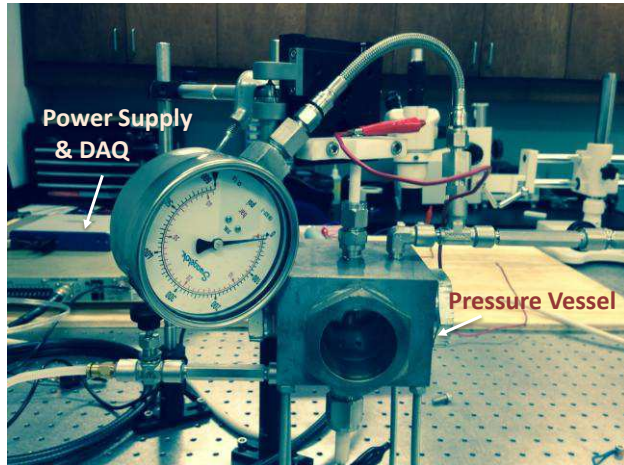


Figure 1. Experimental setup

II. EXPERIMENTAL PROCEDURE

The experimental set up consists of a Spellman 2000 DC power supply connected in series to a 100 k Ω ballast resistor and the powered electrode. The plasma electrodes are enclosed in a high pressure chamber. The plasma chamber is a stainless steel chamber built to withstand high pressure. The chamber contains 4 quartz glass windows for optical diagnostics. Two movable sealed gland electrodes made of copper were used in the experiment. A 1cm disk of 1 cm diameter acts as the cathode. He/N₂ gas is charged into the pressure chamber through a needle valve to obtain the desired pressure. Fresh feed gas is maintained in the pressure chamber via a deliberate small leak. An analog pressure gauge is connected to the chamber to monitor the pressure. A picture of the experimental setup is shown in Figure 1. The VI characterizes curve was obtained by changing the power supply current. The power supply system was driven through a Labview program and a DAQ system. The discharge current is measured across a 100 Ω shunt resistor connected in series to the cathode and the ground.

III. MATHEMATICAL MODEL

The mathematical modelling of the problem is based on the continuum modeling approach due to the high operating pressure. The model consists of conservation equations for electrons, ions, radicals and neutrals. The conservation equations for the electrons and ions are

defined by the species continuity equation with a drift diffusion approximation for the fluxes. The energy conservation equation for the electrons and the gas phase are included in this model. The self consistent electric potential is obtained from the Poisson's equation. In addition, the effect of external circuit parameter was obtained from an external circuit model coupled with the plasma model. The reaction mechanism includes 41 step reactions for helium with nitrogen impurities. 10 species were considered in the simulations; electrons (e), monomer and dimer ions (He⁺, He₂⁺, N₂⁺) electronically excited species (He(2¹S), He(2³S), metastable (He*, He₂*) and neutrals (He, N₂). The reaction mechanism includes the elastic scattering, ionization, excitation and de-excitation, three body recombination, dissociative recombination, charge transfer, molecular ion conversion reactions etc. A details of the mathematical model and the chemical kinetics included in this study is discussed in Ref. [18].

Schematic of the microplasma discharge system studied is shown in Figure 2 and 3. The plasma chamber is connected to the external circuit consisting of a voltage source V_s , a ballast resistor R , and a capacitor C . The capacitor C , also known as parasitic capacitance, is present intrinsically in the wire. In these simulations the inter-electrode separation was fixed at $d = 200 \mu\text{m}$. The simulation was carried out for a two dimensional axisymmetric domain. The schematic of the computational domain is depicted in Figure 3 where 1-2 represents the anode, 3-4 represents the cathode surface and 2-3 is the dielectric wall. The interelectrode distance 1-4 is set to be 200 μm . The mesh of the discharge domain consists of '22500' mapped quad elements. The total number of degrees of freedom was approximately '342168'. A fully implicit backward difference formula (BDF) and a variable time stepping was used for the time integration. The numerical solution was obtained utilizing the Parallel-Sparse Direct Solver.

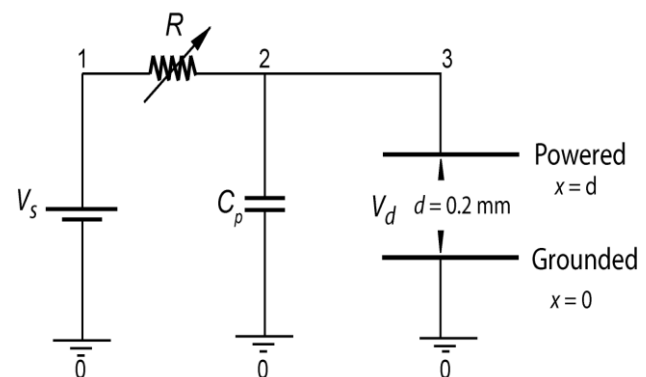


Figure 2. Schematic of the parallel plate plasma glow discharge circuit. The numbers represents the node in the circuit, '0' indicates ground nodes.

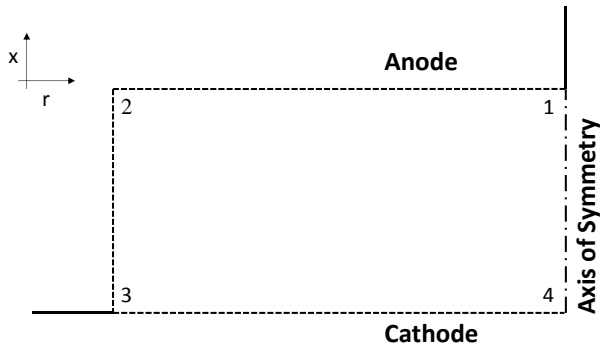


Figure 3. Schematic of the computational domain. The dotted line represents the boundary.

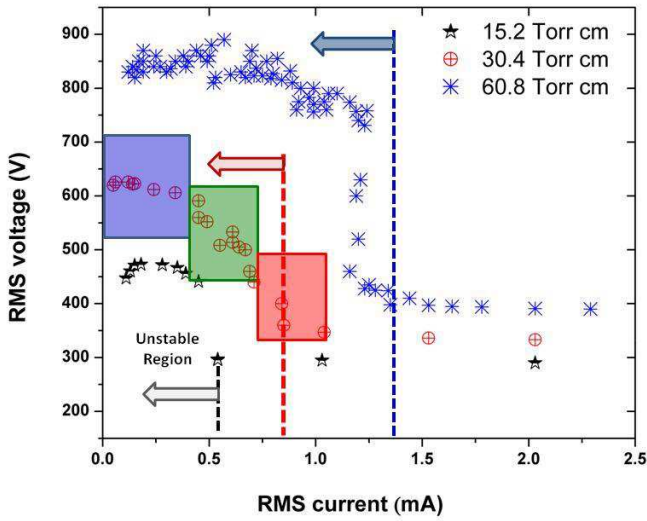


Figure 4. Experimental voltage current characteristics curve for different ‘pd’ values.

IV. RESULTS & DISCUSSION

A. Experimental Results

The voltage current characteristics curve at different pressure is presented in Figure 4. The voltage and current for the oscillatory discharges are presented in terms of their RMS values. The data are for three different pressure: 1 atm, 2 atm and 4 atm. The regions of stable and unstable regions are also denoted. It is interesting to note that the discharge current at which the transition takes place does not scale linearly with ‘pd’. In the negative differential resistance (NDR) region the voltage is found to decrease at two different rates; low and high. At very low currents the discharge voltage decreases very slowly as a function of discharge current. This happens for a current value around 0.1 mA to 0.2 mA depending on pressure (Figure 5(a)). In this range the discharge voltage decreases to ‘zero’ values and increases to 1200 V in two steps. The discharge current also shows large spikes to ~2.0 – 2.5 mA which is followed by a long duration of zero discharge currents. The discharge is

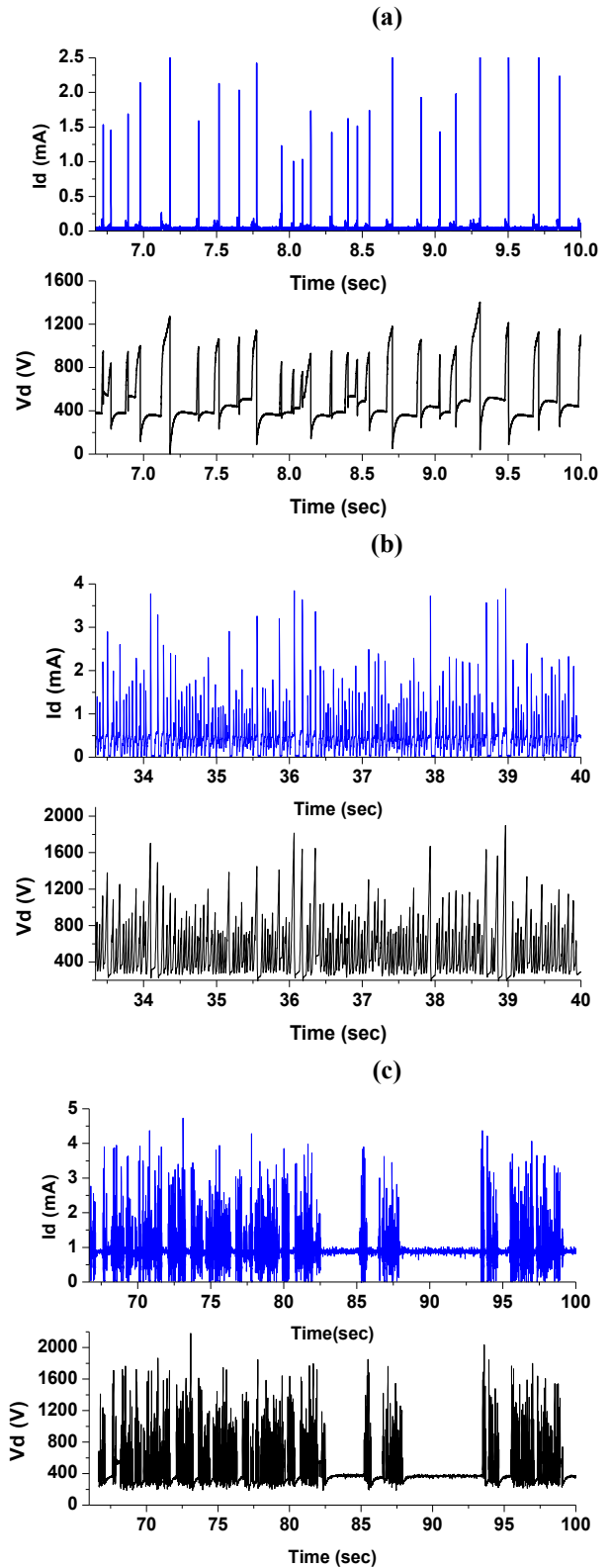


Figure 5. Experimental discharge current and voltage profile for (a) $I_{rms} = 0.12$ mA and $V_{rms} = 602$ V (b) $I_{rms} = 0.6$ mA and $V_{rms} = 515$ V and (c) $I_{rms} = 0.94$ mA and $V_{rms} = 400.35$ V at 30.4 Torr cm.

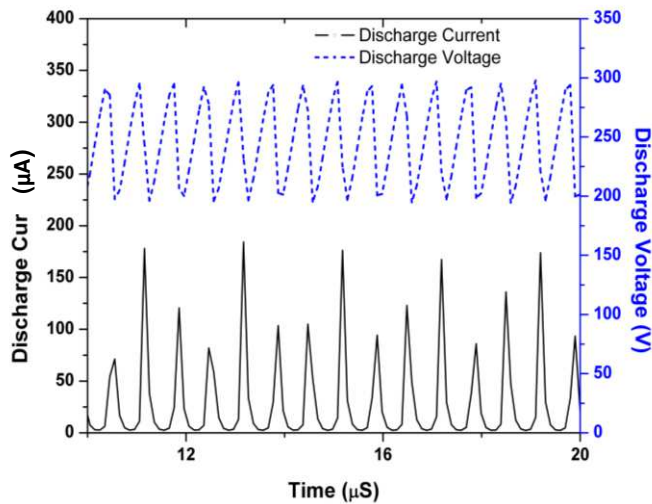


Figure 6. Quasi steady state transient switching of discharge voltage and current for the baseline condition. (900 V power supply, 50 MΩ Ballast resistance, 0.01 pF parasitic capacitance, 15.2 Torr cm)

found to oscillate at low frequency. This low frequency pulsing can be characterized as a relaxation type of oscillation where the discharge goes through complete ionization and neutralization state. As current increases (> 0.2 mA at 30.4 Torr cm), the discharge does not go through a 'zero' current state indicating that the discharge does not go through a complete cycle of initiation and extinction. In this region the rms discharge voltage decreases with current much more rapidly (0.2 mA $< I_d < 0.94$ mA at 30.4 Torr cm). High frequency oscillation is characteristics of this regime as evident in the discharge current and voltage oscillograms (Figure 5(b)). When discharge current is further increased (> 0.94 mA at 30.4 Torr cm), the discharge shows multiple pattern of self pulsing mode. The frequency of oscillation is generally in the MHz ranges (Figure 5(c)). The discharge was observed to happen at different locations on the cathode surface. The high frequency self pulsing mode can be characterized as a free running type oscillation and this pulsing is not visible in naked eyes. At higher current (> 2 mA) a steady normal glow type discharge is attained. In

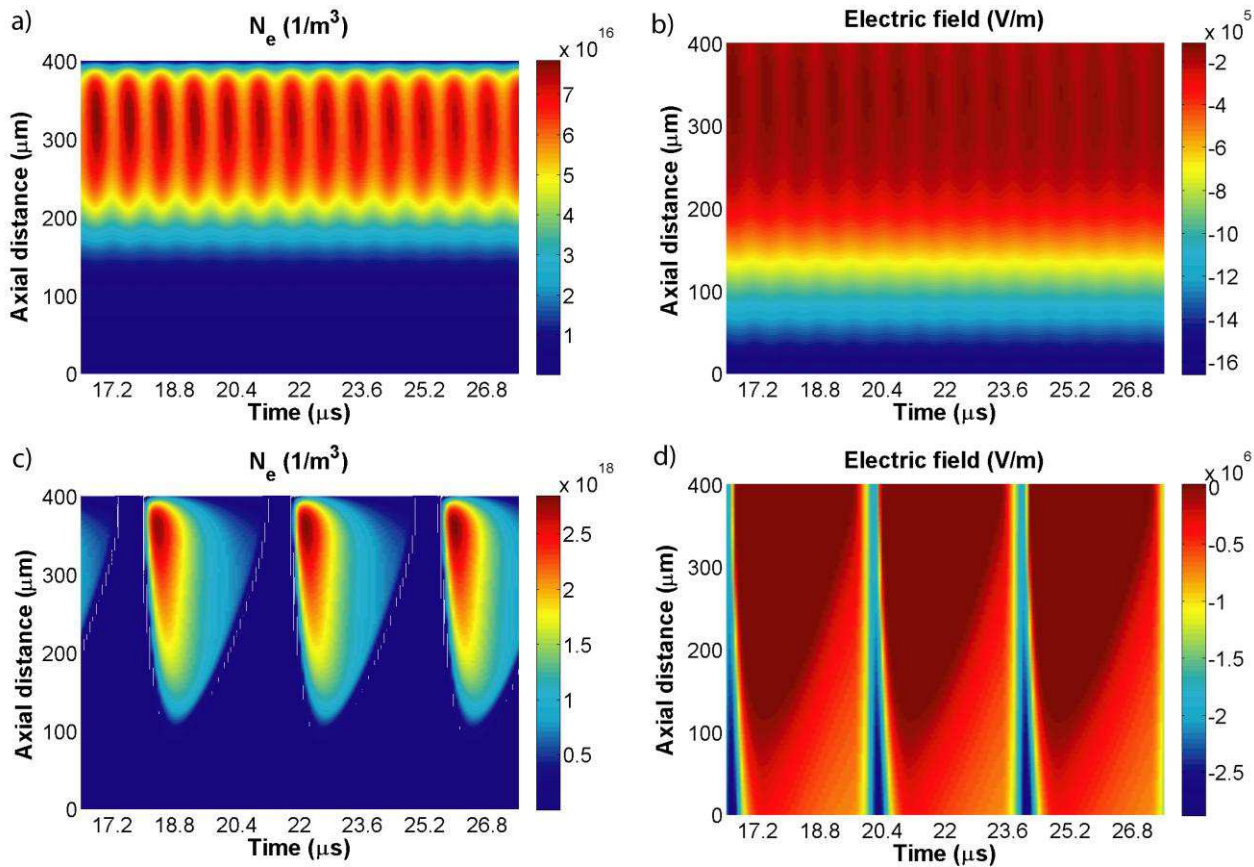


Figure 7. Quasi-steady state spatial-temporal plot at 30.4 Torr cm of (a) Electron number density for high current free running oscillation (maximum value $8 \times 10^{16} \text{ m}^{-3}$) (b) Electric field for high current free running oscillation (maximum value $-16 \times 10^5 \text{ V m}^{-1}$) (c) Electron number density for low current relaxation (maximum value $2.5 \times 10^{18} \text{ m}^{-3}$) and (d) Electric field (maximum value $-2.5 \times 10^6 \text{ Vm}^{-1}$) for low current relaxation oscillations.

the normal region the discharge current increases whereas the discharge voltage remains almost constant.

In the experimental voltage current characteristics (Figure 4) the influence of pressure is also summarized. At higher pressure the unstable region is found to extend to higher discharge currents. As stated earlier $I_{d\text{-transition}}$ does not scale linearly with pressure indicating there may be some non-linear effects that dictates the transition region from stable to unstable discharge modes. The high pressure discharges are characterized by a radial constriction of current and a slower rate of ion mobility. The slower ion mobility makes the high pressure discharge more prevalent to these circuit driven instability.

B. Numerical Results

Numerical simulations were conducted to obtain detailed insight on the different pulsing modes Exemplar numerical results are presented in Figure 6 and 7. Figure 6 presents the temporal evolution of the discharge voltage and current during the quasi-steady pulsing period. The plasma instability is found to develop when the circuit response time (τ_{RC}) becomes higher or comparable to the transient plasma instability time (τ_{trns}) [16, 19]. The comparable higher circuit constant time enables the necessary condition for instabilities which leads to the different type of oscillatory mode. To recognize the different oscillatory modes the spatial-temporal plot of the electron number density and electric field along the center line is for two different currents are presented in Figure 7. At higher current, as shown in Figure 7(a) and 7(b), it is evident that the discharge does not go through a complete extinction process. Even though the electron number density pulsates it never reduces to extreme low densities – the plasma domain always maintains a significant concentration of electrons even between pulses. The fluctuation of the electric field is also minimal at high discharge currents. Since, the plasma does not undergo extinction this type of pulsing can be termed “free running” type of oscillation.. However, if the circuit response time is much higher than the plasma instability time the discharge undergoes full cycle of formation and extinction process as shown in Figure 7(c) and 7(d). This happens at relatively lower current condition and can be distinguished as a relaxation type of oscillation. Similar to the experimental results, the frequency of relaxation oscillation is much lower than the high current free running oscillation. The RMS voltage current characteristic curve is plotted in Figure 8. The model predicts a similar discharge pattern and the predictions are found to qualitatively match the experimental measurements. The experimental discharge voltage was found to be higher than the simulation result. This discrepancy can be attributed to possible limitation in the chemical kinetics and constant secondary electron

emission coefficient (e.g., no electric field dependence) imposed at the cathode boundary.

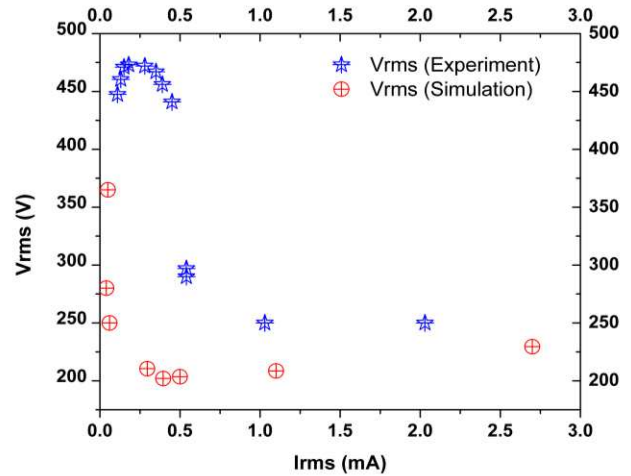


Figure 8. Comparison between the experimental and numerical VI characteristic curve (15.2 Torr cm).

V. CONCLUSION

Self-pulsing micro-discharge operating at atmospheric and higher pressure in a He-N₂ feed gas is studied experimentally and numerically. The self-oscillatory modes is characterized by a repetitive form of discharge voltage and current pulsation when the ion transit time ($\tau_{trns} = d / v_i$) becomes comparable or larger than the external circuit time constant ($\tau_{RC} = RC$) [16, 19]. The modes of oscillation are characterized as low current low frequency relaxation oscillation and high current, high frequency free running oscillation. These oscillatory modes are also depends on the external circuit parameters as well as pressure. The different oscillatory modes are more prevalent at high pressure condition. At higher pressure the oscillations are found to occur at higher discharge currents. The temperature rise during the plasma discharge was insignificant; therefore, this self pulsing mode is not a related to ionization overheating instability rather it is driven by external circuit parameters.

VI. REFERENCES

- [1] Michael A. Lieberman and A. J. lichtenberg, Principles of Plasma Discharges and Materials Processing, 2nd Edition ed., John Wiley & Sons, 2005.
- [2] T. Farouk, B. Farouk, D. Staack, A. Gutsol, A. Fridman, Plasma Sources Science and Technology, 15 (2006) 676.
- [3] D. Staack, B. Farouk, A. Gutsol, A. Fridman, Plasma Sources Science and Technology, 14 (2005) 700.

- [4] A. Fridman and L. A. Kennedy, Plasma Physics and Engineering, 2nd ed., CRC Press, 2011.
- [5] E. Stoffels, A. Flikweert, W. Stoeffls, G. Kroesen, Plasma Sources Science and Technology, 11 (2002).
- [6] G. Fridman, M. Peddinghaus, H. Ayan, A. Fridman, M. Balasubramaniam, A. Gutsol, A. Brooks, G. Friedman, Plasma Chemistry and Plasma Process, 26 (2006) 425-442.
- [7] D. Staack, B. Farouk, A. Gutsol, A. Fridman, Thin film deposition using atmospheric pressure microplasma, in: 34th IEEE International Conference on Plasma Science, IEEE, Albuquerque, New Mexico, 2007, pp. 901-904.
- [8] S.E. Babayan, J.Y. Jeong, V.J. Tu, J. Park, S.G. S., R.F. Hicks, Plasma Sources Science and Technology, 7 (1998) 286-288.
- [9] A. Schutze, J.Y. Jeong, S.E. Babayan, J. Park, G.S. Selwyn, R.F. Hicks, IEEE Trans. Plasma Sci., 26 (1998) 1685-1694.
- [10] T. Farouk, B. Farouk, D. Staack, A. Gutsol, A. Fridman, Plasma Sources Science and Technology, 16 (2007) 619.
- [11] D.D. Hsu, D.B. Graves, Journal of Physics D: Applied Physics, 36 (2003) 2898-2907.
- [12] X. Aubert, G. Bauville, J. Guillon, B. Lacour, V. Puech, A. Rousseau, Plasma Sources Science and Technology, 16 (2007) 23-32.
- [13] T. Deconinck, L.L. Raja, Plasma Processes and Polymers, 6 (2009) 335-346.
- [14] D. Staack, B. Farouk, A. Gutsol, A. Fridman, Journal of Applied Physics, 106 (2009).
- [15] T. Farouk, D.S. Antao, B. Farouk, IEEE Transactions on Plasma Science, (2014) (Accepted in Press).
- [16] R.R. Arslanbekov, V.I. Kolobov, Journal of Physics D: Applied Physics, 36 (2003) 2986.
- [17] COMSOL Multiphysics, in: Multiphysics Reference Guide for COMSOL 4.3, Burlington, MA, USA, 2013.
- [18] R. Mahamud, T. Farouk, Journal of Physics D: Applied Physics (in Review).
- [19] A.A. Kudryavtsev, L.D. Tsendin, Technical Physics Letters, 28 (2002) 1036-1039.